

UC Davis

UC Davis Previously Published Works

Title

Microarray analyses of closely related glycoforms reveal different accessibilities of glycan determinants on N-glycan branches.

Permalink

<https://escholarship.org/uc/item/48p3f5xv>

Journal

Glycobiology, 30(5)

ISSN

0959-6658

Authors

Li, Lei
Guan, Wanyi
Zhang, Gaolan
et al.

Publication Date

2020-04-20

DOI

10.1093/glycob/cwz100

Peer reviewed

Glycan Recognition
Editor's Choice

Microarray analyses of closely related glycoforms reveal different accessibilities of glycan determinants on *N*-glycan branches

Lei Li^{1,2}, Wanyi Guan^{2,†}, Gaolan Zhang², Zhigang Wu^{2,‡}, Hai Yu², Xi Chen³ and Peng G Wang^{2,§}

²Department of Chemistry, Georgia State University, Atlanta, GA 30303, USA and ³Department of Chemistry, University of California, One Shields Avenue, Davis, CA, 95616, USA

¹To whom correspondence should be addressed: e-mail: lli22@gsu.edu

[†]Present address: College of Life Science, Hebei Normal University, Shijiazhuang, Hebei 050024, China

[‡]Present address: College of Bioscience and Bioengineering, Hebei University of Science and Technology, Shijiazhuang, Hebei 050018, China

[§]Present address: Department of Chemistry, Southern University of Science and Technology, Shenzhen 518055, China

Received 15 March 2019; Revised 27 November 2019; Editorial Decision 27 November 2019; Accepted 2 December 2019

Abstract

Glycans mediate a wide variety of biological roles via recognition by glycan-binding proteins (GBPs). Comprehensive knowledge of such interaction is thus fundamental to glycobiology. While the primary binding feature of GBPs can be easily uncovered by using a simple glycan microarray harboring limited numbers of glycan motifs, their fine specificities are harder to interpret. In this study, we prepared 98 closely related *N*-glycoforms that contain 5 common glycan epitopes which allowed the determination of the fine binding specificities of several plant lectins and anti-glycan antibodies. These *N*-glycoforms differ from each other at the monosaccharide level and were presented in an identical format to ensure comparability. With the analysis platform we used, it was found that most tested GBPs have preferences toward only one branch of the complex *N*-glycans, and their binding toward the epitope-presenting branch can be significantly affected by structures on the other branch. Fine specificities described here are valuable for a comprehensive understanding and applications of GBPs.

Key words: chemoenzymatic synthesis, glycan-binding protein, glycoform, microarray, *N*-glycan

Introduction

Glycan-binding proteins (GBPs), which bind specific glycan (or carbohydrate) structures but have no enzymatic activity, decipher the glycan code of cell surfaces and translate information obtained from glycan recognition into functions during various biological processes, including signal transduction, cell adhesion, immune recognition, microbial infection, etc. (Taylor et al. 2015) Given their specific glycan-binding properties, many GBPs (especially plant lectins) have been extensively employed in glycobiology as detection and analysis tools. (Hendrickson and Zherdev 2018) For example, *Sambucus nigra*

lectin (SNA) and *Maackia amurensis* lectin I (MAL-I) are routinely used to identify α 2,6- and α 2,3-linked sialic acid (Sia), respectively, and concanavalin A (ConA) is a lectin commonly used to enrich tryptic *O*-mannosyl peptides. Lectin microarrays have also been developed for rapid analysis of protein glycopatterns and glycomes (Pilobello et al. 2005, 2007). On the other hand, immunotherapies targeting human GBPs and their ligands offer promising therapeutic strategies in combating tumor and other diseases. (Hudak and Bertozzi 2014; Rodriguez et al. 2018) Such applications rely on a complete knowledge of GBPs and their related glycan ligands.

Other than the minimal glycan-recognition motif that defines the primary specificity of a GBP, recent studies revealed that its binding could be significantly affected by the way the motif is presented, including the length of the underlining structures, the location of the branch, the modification and substituents on the neighboring structures, etc. (Taylor and Drickamer 2009; Wang et al. 2013, 2018; Wu et al. 2016) Such fine details are valuable for a comprehensive understanding of GBPs and their applications. While the primary binding feature can be revealed readily using a small number of simple glycoforms with the powerful glycan microarray technology, the fine specificity is harder to determine, which would require libraries of closely related structures. Fewer efforts have been put forth for this purpose. Haab and coworkers described an “outlier-motif” algorithm for automated extraction and systematic analysis of existing glycan array datasets, which uncovered substructure patterns that could provide more binding details of lectins (Maupin et al. 2012). They further reported another strategy to elucidate higher-level lectin binding preference by treating glycan microarray with exoglycosidases before binding assays (Klamer et al. 2017). Other valuable software/algorithms have also been developed to mine refined glycan substructures that influence protein-glycan interactions (Xuan et al. 2012; Kletter et al. 2013; Agravat et al. 2014; Zhao et al. 2015; Grant et al. 2016). All these algorithms are based on systematic analyses of existing microarray result datasets, which should be done with caution concerning diversity on array platforms, conjugation or immobilization strategies and processing protocols (Padler-Karavani et al. 2012; Wang et al. 2014).

Microarray profiling using glycans with similar structural features represents an alternative and more reliable strategy to uncover fine binding specificities of GBPs. For example, microarray analysis using a library of extended airway glycans containing a terminal *N*-acetylneuraminic acid (Neu5Ac) revealed that currently circulating human H3N2 influenza viruses had evolved to adopt a preference toward branched glycan structures with extended poly-*N*-acetylglucosamine (poly-LacNAc) chains (Peng et al. 2017). We previously synthesized a number of symmetric bi-antennary *N*-glycans with tandem epitopes, and microarray analyses revealed fine preferences of GBPs toward terminal and internal epitopes (Wu et al. 2016). *N*-Glycan positional isomers were also prepared recently for fine specificity mining (Echeverria et al. 2018; Gao et al. 2019). It was also shown that SNA recognized a minimal Neu5Ac- α 2,6-LacNAc determinant presented at the terminus of the α 1,3-Man branch but not the α 1,6-branch of *N*-glycans (Smith et al. 2010). We recently synthesized a set of *O*-mannosyl glycans containing closely related structures, and microarray analyses again revealed fine details besides the primary features recognized by lectins and anti-glycan antibodies (Wanget al. 2018). Nevertheless, fine details obtained from all reported cases are limited, focusing on a narrow range of examples and are just the tip of the iceberg. Obtaining a large set of structurally related complex glycans will help to get a comprehensive view of the fine specificities of GBPs and to speed up their applications.

We sought to study the fine specificities of commonly applied GBPs toward glycan determinants that are presented on *N*-glycans. Specifically, in the present study, we report the preparation of a unique set of closely related glycoforms that differ at the monosaccharide level. Microarray profiling using these structurally well-defined glycoforms revealed fine specificities of GBPs, including their preference toward branch, modifications on underlying glycans, and more.

Results

Preparation of closely related glycoforms and construction of the glycan microarray

N-Glycans, which share a signature core pentasaccharide structure (Man₃GlcNAc₂), are covalently attached to proteins at asparagine (Asn) residues via an *N*-glycosidic bond. Naturally occurring *N*-glycans are inherently complex and diverse with variations on the number of antennae and glycan determinants. Interactions between GBPs and asymmetrically branched *N*-glycans follow a context-dependent recognition manner, (Wang et al. 2013) and glycan asymmetry was believed to play a regulatory role in such interactions (Shivatare et al. 2016). To identify fine glycan-recognition specificities of GBPs, we prepared 68 asymmetric and symmetric *N*-glycans presenting five major glycan determinants, (Li et al. 2015) including LacNAc (LN, Gal- β 1,4-GlcNAc), Neu5Ac- α 2,3-LacNAc (3'SLN), Neu5Ac- α 2,6-LacNAc (6'SLN), Lewis X [Le^x, Gal- β 1,4-(Fuc- α 1,3-)GlcNAc] and sialyl-Le^x [sLe^x, Neu5Ac- α 2,3-Gal- β 1,4-(Fuc- α 1,3-)GlcNAc] epitopes (Table I, Figure S1, glycans 1–68). This well-defined glycan library covers all possible bi-antennary *N*-glycans presenting the five epitopes, including 28 pairs of branch positional isomers. For example, as shown in Figure 1A, glycans 16, 22, 40, 44, 47, 66 and 67 share the 6'SLN epitope on the α 1,3-Man branch, but differ on the α 1,6-Man branch, with systematic increase of the number of monosaccharides from 0 to 5. In contrast, their corresponding branch isomers 28, 34, 56, 60, 63, 50 and 51 share the same epitope on the α 1,6-Man branch but differ on the other branch. Such closely related glycoforms provide an ideal set of standards to probe fine specificities of GBPs.

Additionally, 10 *N*-glycolylneuraminic acid (Neu5Gc)-terminated *N*-glycans were prepared to study the binding preferences of GBPs toward the two most abundant sialic acid forms: Neu5Ac and Neu5Gc. Among these, 69–71 were prepared previously, (Li et al. 2015) and 72–78 were enzymatically synthesized following similar one-pot two-enzyme systems (Supplementary Information I). The glycan library also contains four multiantennary and five core-fucosylated structures (Figure 1B, 79–87), (Calderon et al. 2016, 2017) as well as three additional *N*-glycans (Figure 1B, 88–90) to study the influence of corresponding glycan modifications on protein-glycan interactions. *N*-glycans 88 and 89 were enzymatically synthesized starting from 14 and 54, catalyzed by bovine α 1,3-galactosyltransferase (β 3GalT) (Fang et al. 1998) and *Neisseria meningitidis* α 1,4-galactosyltransferase (NmLgtC), (Zhang et al. 2002) respectively. Interestingly, unlike β 3GalT-catalyzed reaction that showed a 100% conversion, only less than 5% of 54 was converted to 89 in the NmLgtC-catalyzed reaction, suggesting that the large underlying *N*-glycan core structure is unfavorable to NmLgtC, consistent with our previous report (Ban et al. 2012).

All *N*-glycans, together with 8 ganglioside glycans that contain the five epitopes (Figure 1B), (Yu et al. 2016) are free reducing oligosaccharides. They were individually synthesized via chemoenzymatic approaches, purified by HILIC-HPLC, and characterized by NMR and HRMS (Supplementary information I) (Li et al. 2015; Calderon et al. 2016, 2017). The synthesis of the desired structures (e.g., linkages and anomeric configurations) was controlled by the well-established step-wise synthetic strategy as well as substrate specificities of corresponding glycosyltransferases. All glycosylation products were further tagged with 2-amino-*N*-(2-aminoethyl)-benzamide (AEAB), (Song et al. 2009) with high yield and further purified

Table 1. Structures of 81 out of 98 glycans presented on the microarray. The symbolic nomenclature for glycans is shown. A pair of branch isomers defined as two *N*-glycans (e.g., N1 and N2) where the α 1,3-Man branch of N1 and the α 1,6-Man branch of N2 share one glycan motif, meanwhile, the α 1,6-Man branch of N1 and the α 1,3-Man branch of N2 share another glycan motif

Type	Structure	Branch A	Branch B	Glycan No.	Branch Isomer
Symmetric bi-antennary		GlcNAc		1	
		LN		2	
		3'SLN		3	
		6'SLN		4	
		Le ^x		5	
		sLe ^x		6	
		3'GLN		77	
6'GLN		78			
Hybrid type		H		90	
		GlcNAc		7	
		LN		8	
		3'SLN	Not Applicable	9	
		6'SLN	Not Applicable	10	
		Le ^x	Not Applicable	11	
		sLe ^x	Not Applicable	12	
3'GLN		69			
6'GLN		70			
gLe ^x		71			
Mono-antennary		GlcNAc		13	25
		LN		14	26
		3'SLN		15	27
		6'SLN		16	28
		Le ^x	Not Applicable	17	29
		sLe ^x	Not Applicable	18	30
		3'GLN		72	
		6'GLN		73	
gLe ^x		74			
				88	
Asymmetric bi-antennary		GlcNAc	PerGlcNAc	37	53
		LN	GlcNAc	38	54
		3'SLN	GlcNAc	39	55
		6'SLN	GlcNAc	40	56
		Le ^x	GlcNAc	41	57
		sLe ^x	GlcNAc	42	58
		3'SLN	LN	43	59
6'SLN	LN	44	60		
Le ^x	LN	45	61		
sLe ^x	LN	46	62		
6'SLN	3'SLN	47	63		
Le ^x	3'SLN	48	64		
sLe ^x	3'SLN	49	65		
Le ^x	6'SLN	50	66		
sLe ^x	6'SLN	51	67		
sLe ^x	Le ^x	52	68		
3'GLN	GlcNAc	75			
6'GLN	GlcNAc	76			
GlcNAc				89	

Keys:

Glc	Gal	Man	L-Fuc	Neu5Ac	Neu5Gc
Kdn	GlcNAc	PerGlcNAc, Peracetylated GlcNAc			
3'SLN	6'SLN	3'GLN	6'GLN		
LN, LacNAc	Le ^x	sLe ^x	gLe ^x		

by a second porous graphitic carbon-HPLC to ensure homogeneity. After confirmed by mass spectrometry, AEAB-labeled glycans were printed by noncontact printing on *N*-hydroxysuccinimide (NHS)-activated glass slides at equal molarities (Figure S2). These steps ensured the comparability of the structures for microarray analysis. The guidelines set forth by the MIRAGE (Liu et al. 2016) were followed during sample preparation, microarray printing, analysis and data processing.

Fine specificity of Sia-binding lectins SNA and MAL-I

SNA and MAL-I have been extensively employed to probe Sia-containing glycans. SNA recognizes α 2,6-linked Sia with a preference to the 6'SLN motif, whose interactions can be greatly influenced by the underlying structures, (Padler-Karavani et al. 2012) whereas MAL-I binds α 2,3-linked Sia, with trisaccharide 3'SLN as the reported minimal recognition motif (Wang and Cummings 1988; Song et al. 2011). Our results showed that both lectins prefer Neu5Gc-containing glycans (Figure 2A, 70, 73, 76, 78 for SNA; Figure 2B, 69, 72, 75, 77 for MAL-I) over their Neu5Ac-containing counterparts (Figure 2A, 10, 16, 40, 4 for SNA; Figure 2B, 9, 15, 39, 3 for MAL-I), indicating that the additional hydroxyl group on C5 of Neu5Gc may play a role in the SNA/MAL-I recognition. On the other hand, SNA exhibited an apparent α 1,3-Man branch preference as previously reported (Smith et al. 2010). For example, the relative fluorescence units (RFU) of SNA binding to *N*-glycans with 6'SLN on the α 1,3-Man branch (16, 22, 40, 44, 47, 66, 67) are 3–6 folds higher than those with their branch isomers (28, 34, 56, 60, 63, 50, 51) (Figure 2A), whereas MAL-I has a strong binding preference to the 3'SLN on the α 1,6-Man branch, reflected by much higher RFU with 27, 33, 47, 48, 55, 59 compared to those with their branch isomers 15, 21, 63, 64, 39 and 43 (Figure 2B). Another noticeable difference of the two Sia-binding lectins is that SNA prefers complex *N*-glycans over linear structures such as glycan 97 (Figure 2A), whereas MAL-I prefers linear structures (93, 94, 95, 96) over branched *N*-glycans (Figure 2B). Most recently, Gao and coworkers reported weak binding of MAL-I toward symmetric Gal-terminating *N*-glycans, (Gao et al. 2019) which is confirmed in this study (2, 79). Using this asymmetric *N*-glycan library, an additionally binding specificity observed is that MAL-I binds Gal-terminated epitopes only on the α 1,6-branch (e.g., 15, 26, 32, 45, 54, and 86) but not any other branches (e.g., 14, 20, 38, 61, and 81–83) (Figure 2B). Most interestingly, MAL-I binds weakly to biantennary *N*-glycans presenting the same ligand (LN or 3'SLN) at both branches (2, 3), but the strongest binding to the asymmetric 59 (with LN on the α 1,3-Man branch and 3'SLN on the α 1,6-Man branch) among all *N*-glycans tested, suggesting that the lectin may have two different ligand-binding pockets that favor the epitope presentation in 59 (e.g., its branch isomer 43 showed only 1/3 of binding intensities for 59).

When comparing the bindings toward glycans that share a 6'SLN-containing branch, a gradually decreased influence by motifs on the opposing branch can be concluded (3'SLN > Le^x \approx LacNAc > GlcNAc), for example, as shown in Figure 2A, RUF with 47 < 66 \approx 44 < 40 (the glycans share the 6'SLN on the α 1,3-Man branch) and RUF with 63 < 50 \approx 60 < 56 (the glycans share the 6'SLN on the α 1,6-Man branch). A similar binding pattern was observed at low concentrations of SNA (e.g., 1 μ g/mL, Supplementary Information II). These results suggested that unlike β 1,4-galactosylation or α 2,3-sialylation, α 1,3-fucosylation on the opposing branch may not affect the binding of SNA toward the

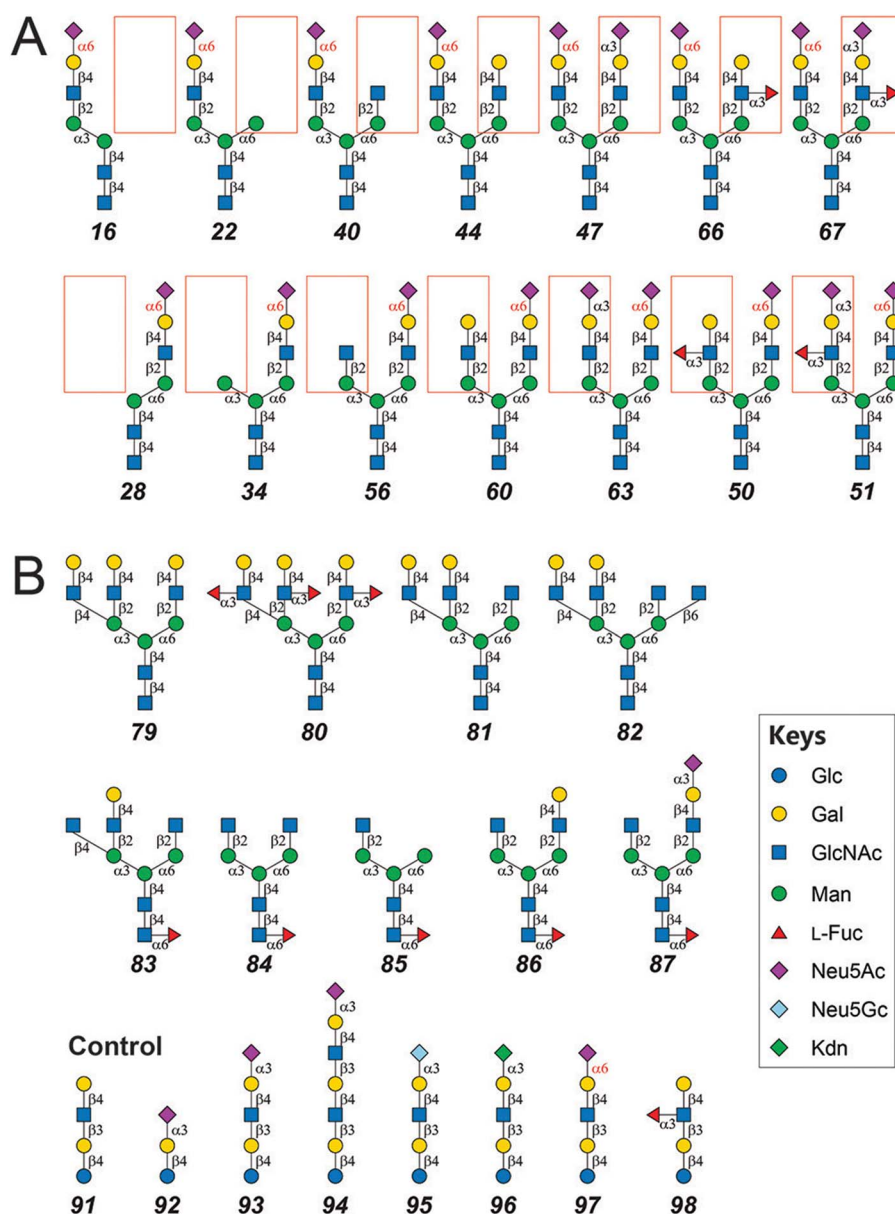


Fig. 1. Examples of *N*-glycans that share one identical branch but differ in the other (highlighted in red rectangles) (A), and structures of multiantennary, core-fucosylated *N*-glycans and 8 linear oligosaccharides as control (B). The symbolic nomenclature for glycans is shown.

6'SLN-containing branch. However, bindings of SNA to 6'SLN on one branch of human milk oligosaccharides (HMOs) were found negatively affected by α 1,3-fucosylation on the opposing branch, (Klamer et al. 2017) probably due to disparate spatial conformations of HMOs (β 1,2-GlcNAc and β 1,6-GlcNAc branches). In some cases, different branch configurations could abolish bindings, as we observed for both SNA and MAL-1 toward an array of 6'SLN- and 3'SLN-containing *O*-mannosyl glycans (Wang et al. 2018) (data not shown). Similarly, it is also observed that structures on the opposing branch could also affect MAL-I binding toward the 3'SLN-containing branch, but more complicated due to nonspecific recognition toward the LacNAc motif.

This microarray shares seven symmetric bi-antennary *N*-glycans (2, 3, 4, 5, 6, 77 and 78) with our previously reported platform, (Wu et al. 2016) on which glycans are linked to Asn instead of AEAB. Binding activities of SNA and MAL-I (as well as ECL, anti-CD15 and

anti-CD15s antibodies) toward these glycans are consistent on the two platforms, with the only exception that MAL-I exhibited very weak binding toward 3 in this study, whereas a moderate binding activity toward the same *N*-glycan attached to Asn (BA-04) was observed previously (Wu et al. 2016). Such observations suggest that presenting formats can affect binding activities of certain GBPs toward certain glycans as concluded previously (Padler-Karavani et al. 2012). Thus, binding specificities concluded in current platform may not well applicable to other platforms.

Fine specificity of LacNAc-binding lectins ECL and RCA-I

Erythrina cristagalli lectin (ECL) and *Ricinus communis* agglutinin (RCA-I) recognize terminal Gal residues, with a strong preference to type II structures (LacNAc, Gal- β 1,4-GlcNAc), and modifications on the Gal residue can significantly influence the binding

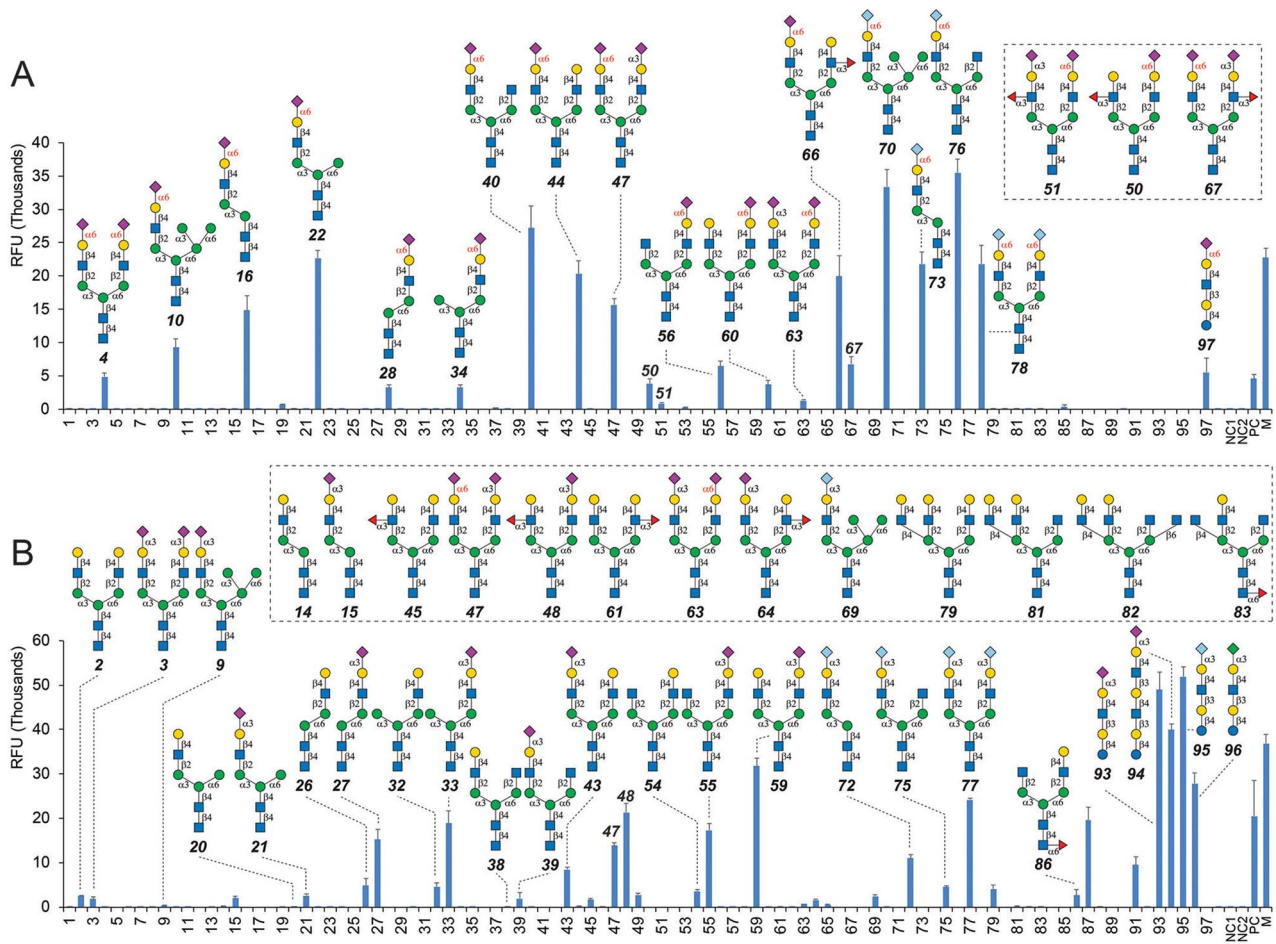


Fig. 2. Selective recognition of *N*-glycans bearing terminal Sia by SNA (A) and MAL-1 (B). The x-axis shows the glycans, and the y-axis shows the relative fluorescence. Readout by Cy5-streptavidin (5 g/mL), NC1 = printing buffer, NC2 = 100 M AEAB in printing buffer, PC = 0.01 mg/mL biotin-PEG-amine, M = Marker (0.01 mg/mL Cy3-conjugated anti-Human IgG + 0.01 mg/mL Alexa647-conjugated anti-Human IgG).

(Itakura et al. 2007; Wu et al. 2007). Such features were confirmed by current microarray, as both lectins showed strong bindings to *N*-glycans with terminal LacNAc motifs (Figure 3, glycans 8, 14, 20, 26, 32, 38). Surprisingly, neither lectins exhibited significantly increased binding activity to multiantennary LacNAc-containing structures (2, 79, 81, 82), suggesting that the spatial conformation of these structures may only allow proper recognition of one LacNAc motif. In terms of branch preference, ECL slightly favors the α 1,3-Man branch (Figure 3A, RFU with 8, 14, 20 > 26, 32), while RCA-I exhibited a stronger preference to the same branch (Figure 3B, RFU with 8, 14, 20 >> 26, 32). Such specificity was also observed against a library of branched *O*-mannosyl glycans (Wang et al. 2018). Neither GBP could tolerate α 2,3-sialylation (3, 9, 15, 21, 27, 33, 39), (Gao et al. 2019) α 1,3-fucosylation (5, 11, 17, 23, 29, 35, 41), or α 1,3-galactosylation (88). On the other hand, while α 2,3-sialylation could also block the binding of ECL, it exhibited a more complicated modulation for RCA-I, with limited influence toward LacNAc on the favorable α 1,3-Man branch (RFU with 8, 14, 20, 38 are slightly higher than those with their α 2,6-sialylated forms 10, 16, 22, 40, and 76), but significant negative effect on binding toward LacNAc on the unfavorable α 1,6-Man branch (28, 34, 56) as well as a linear glycan 97 (Figure 3B).

Lastly, ECL and RCA-I exhibited different patterns concerning the influence of modifications on the opposing branch. A clear negative

gradual effect ($sLe^x \approx 6^*SLN \approx 3^*SLN > Le^x > GlcNAc$) was observed for ECL (RFU with 62 \approx 60 \approx 59 < 61 < 38, Figure 3A), whereas RCA-I showed comparable binding activities toward *N*-glycans sharing one LacNAc-containing branch (e.g., glycans 8, 14, 20, 38, 59–62 share the α 1,3-Man branch, and glycans 26, 32, 43, 45, 46 share the α 1,6-Man branch, Figure 3B). Collectively, ECL has a very strict requirement toward unmodified the LacNAc motif on *N*-glycans, whereas RCA-I could well tolerate α 2,6-sialylation on the α 1,3-Man branch, as well as large structures on the opposing branch of *N*-glycans.

Fine specificity of man-binding lectins ConA and GNL and other lectins

Given the high affinity and a quite broad specificity to α -linked Man-containing glycans, ConA has been widely used as an analytical and enriching reagent in glycomics (Kuno et al. 2005; Hirabayashi et al. 2015; Zhang et al. 2016; Zou et al. 2017). The lectin is known to bind biantennary and high-mannose *N*-glycans and could accommodate nonreducing terminal α 2,3/6-sialylation (Porter et al. 2010; Gao et al. 2019). Our results revealed Man- α 1,6-(Man- α 1,3-)Man trisaccharide as a minimum ligand for ConA, and the binding can be significantly affected by further glycosylation on Man residues. It could not recognize structures lacking either α 1,3-Man (26–30)

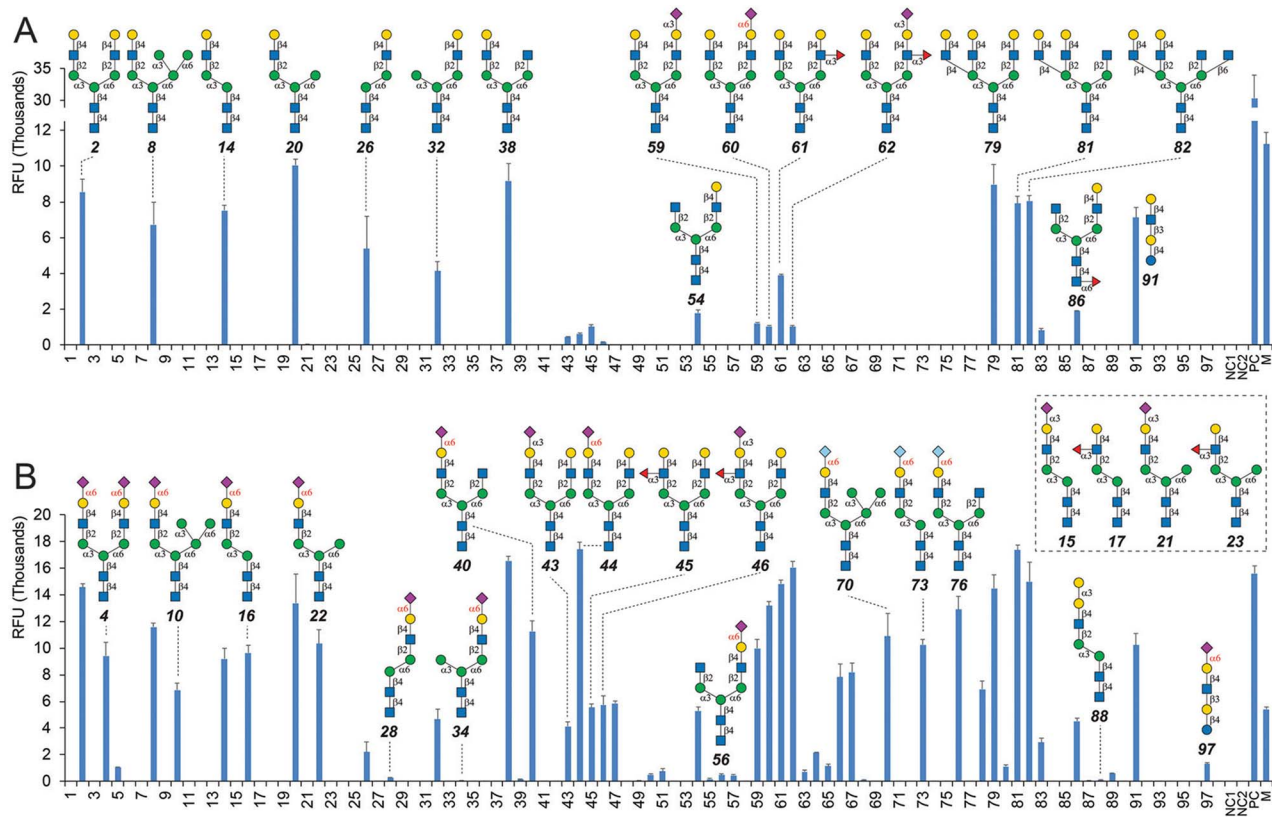


Fig. 3. Selective recognition of *N*-glycans bearing LacNAc disaccharide by ECL (A) and RCA-I (B). Readout by Cy5-streptavidin (5 g/mL).

or α 1,6-Man (14–18, 88) (Figure 4A). GNL recognizes the Man- α 1,3-Man motif, (Shibuya et al. 1988) which is confirmed herein by apparent bindings toward glycans 13–17 but not 25–29 which contain a Man- α 1,6-Man motif (Figure 4B). An additional α 1,6-Man can slightly increase the binding of GNL (19–23). Besides, sialylation and/or α 1,3-fucosylation on either α 1,3-Man or α 1,6-Man branch can reduce (in certain cases, abolish) the binding of GNL (Figure 4B, 19–24, 54–58). Comparing with ConA, GNL exhibited much lower overall binding activity toward *N*-glycans, with an optimal concentration of 10 μ g/mL. As shown in Figure 4A, ConA exhibited much lower binding intensities toward 7 and 90 comparing with those toward 19 and 31, suggesting that the Man- α 1,6-(Man- α 1,3-)Man trisaccharide on the α 1,6-Man branch of *N*-glycans cannot be recognized by ConA, and could significantly reduce its binding to the core Man- α 1,6-(Man- α 1,3-)Man trisaccharide. Another noticeable feature is that ConA could not tolerate galactosylation on an additional β 1,4-GlcNAc branch (79, 80, 82), the same as a recent report (Gao et al. 2019).

We also investigated fine specificities of the Fuc-binding *Aleuria aurantia* lectin (AAL) and the GlcNAc-binding *Griffonia simplicifolia* lectin (GS-II) using this array. As shown in Figure S3, AAL bound to all Fuc-containing glycans (α 1,3-Fuc or α 1,6-Fuc) with high binding activity at concentrations as low as 0.1 μ g/mL. An interesting observation is that α 2,3-sialylation on the same branch of the α 1,3-Fuc can reduce the binding by 44–61% (Figure S3). In addition, glycans with multiple Fuc residues on separate branches (5, 6, 52, 68, 80) did not display apparent higher binding signals, which is different from the fine specificity of AAL toward HMOs, (Klamer et al. 2017). GS-II recognizes nonreducing terminal GlcNAc residues, (Zhu et al. 1996)

as shown in Figure S4. A preference of GS-II toward the α 1,3-Man branch was observed (even though with pretty weak bindings), as RFU with 13 and 19 are 4–5 times of those of 25 and 31. It is worth to note that core-fucosylation did not exhibit apparent influence in bindings of all tested lectins, probably because such a modification is spatially far away from their recognized ligands.

Selective recognition of (s)Le^x-containing *N*-glycans by anti-CD15(s) antibodies and CTB

The anti-CD15 antibody specifically recognizes terminal Le^x epitopes, and modifications on the Gal residues will completely block the binding (Wu et al. 2016). Our previous results using symmetric bi-antennary *N*-glycans arrays and array data published by Consortium for Functional Glycomics (CFG) highlighted possible negative effects of the core-pentasaccharide (Man₃GlcNAc₂) on bindings (Wu et al. 2016). Similar results were observed in this study, e.g., anti-CD15 antibody exhibited no or only neglectable bindings toward 5, 11, 41, 45, 48, 50, 57, 61, 64, 66 and 80 (Figure 5A). However, it exhibited strong bindings to glycans 23 and 35 (which contain Man₃GlcNAc₂ but lack further glycosylation) at the same level as the linear Le^x-containing glycan 98, suggesting that the negative effect may be caused by opposing branches instead of Man₃GlcNAc₂ of *N*-glycans. One Man residue on the opposing branch (23, 35) can be tolerated by the anti-CD15 antibody, while the attachment of another GlcNAc (41, 57) or more residues will greatly affect or abolish the binding. The anti-CD15s antibody recognizes sLe^x epitopes, but no binding was observed toward *N*-glycans with two sLe^x epitopes directly linked to the core-pentasaccharide

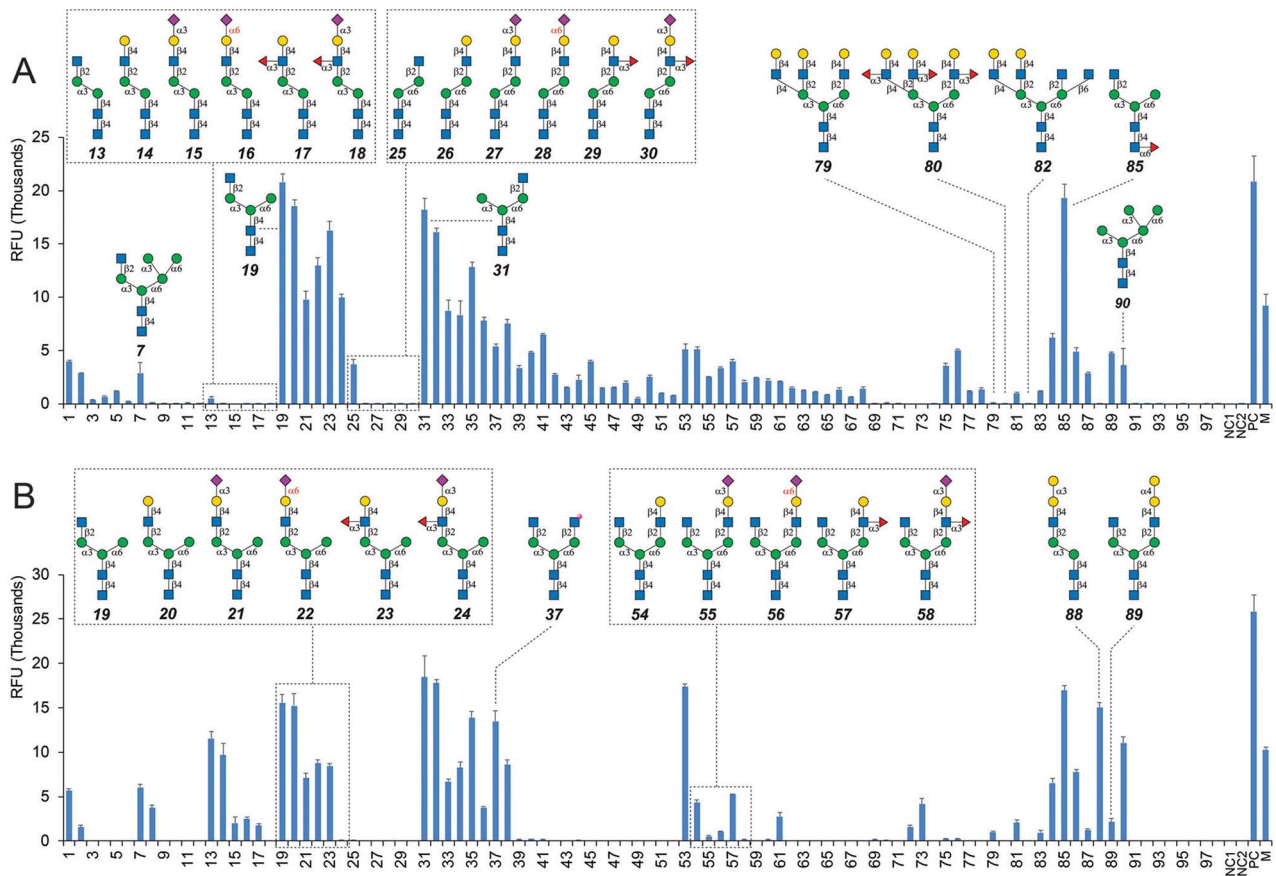


Fig. 4. Selective recognition of *N*-glycans by ConA (A) and GNL (B). Readout by Cy5-streptavidin (5 g/mL).

(Wu et al. 2016). Our results showed that the antibody bound *N*-glycans lacking one branch (18, 24, and 30) with high activities, and certain bi-antennary *N*-glycans (36, 42, 46, 49, 51, and 52) with moderate to low activities (Figure 5B), again suggesting that it is the opposing branch that affected bindings instead of the core-pentasaccharide $\text{Man}_3\text{GlcNAc}_2$.

In addition, higher RFU with 17, 23, and 41 than those with their branch isomers 29, 35, and 57 (Figure 5A) were observed, suggesting that the anti-CD15 antibody slightly favors the α 1,3-Man branch. The anti-CD15s antibody also exhibited a preference to the α 1,3-branch, as RFU with *N*-glycans containing the sLe^x epitope on the α 1,3-branch (24, 42, 46, and 49) are higher than those with their branch isomers (36, 58, 62, and 65), with the exception of 18/30 (Figure 5B). Nevertheless, our results proved that both antibodies prefer *N*-glycans with only one branch, and the extension of the opposing branch can significantly affect their bindings.

It was recently reported that the B subunit of *Vibrio cholera* toxin (CTB) could not only recognize ganglioside GM1 with high affinity, (Kim et al. 2012) but also bind fucosylated cell surface glycoproteins on normal human intestinal epithelia (Wands et al. 2015). As shown in Figure S5, at a high concentration of 50 $\mu\text{g/mL}$, CTB only exhibited moderate binding to LNFP III (98) among all glycans tested. Interestingly, it showed weak bindings to 4 *N*-glycans, 29, 30, 35 and 36, which share the same α 1,6-Man branch (Le^x or sLe^x) but lack the α 1,3-branch. It is possible that (s)Le^x or similar epitopes on glycoproteins may be responsible for CTB binding and play a role in cholera pathogenesis.

Summary

A comprehensive understanding of GBPs and interactions with their ligands can benefit both fundamental research and potential applications. We analyzed a panel of GBPs using a specific glycan microarray that contains 98 closely related glycoforms and branch isomers, revealing common features concerning their fine specificities as summarized in Table II. With the analysis platform we used, all tested GBPs except for AAL have preferences toward one branch of bi-antennary *N*-glycans, which were also observed previously toward branched *O*-mannosyl glycans (Wang et al. 2018) and HMOs (Klamer et al. 2017). SNA, ECL, RCA-I, GS-II and anti-CD15(s) antibodies prefer ligands presented on the α 1,3-Man branch, whereas MAL-I and CTB prefer ligands on the α 1,6-Man branch. Given the common multiantennae property of major mammalian glycans (e.g., *N*-glycans, *O*-glycans and HMOs), it may be a critical modulator of protein-glycan interactions which should be carefully considered in related researches. Worth noting that for all GBPs tested, the presence of multiple ligands on separate branches will not increase the binding activity, but in many cases confer negative impact. A possible explanation would be that one GBP molecule may be only able to recognize one specific ligand, and other ligands on opposing or adjacent branches do not serve as a binder, but instead behave as a steric effector.

While it is well accepted that the underlying structures and modifications of the glycan ligand can modulate bindings, the influence by structures on opposing branches of *N*-glycans has been rarely discussed (Klamer et al. 2017; Wu et al. 2017; Gao et al. 2019). As

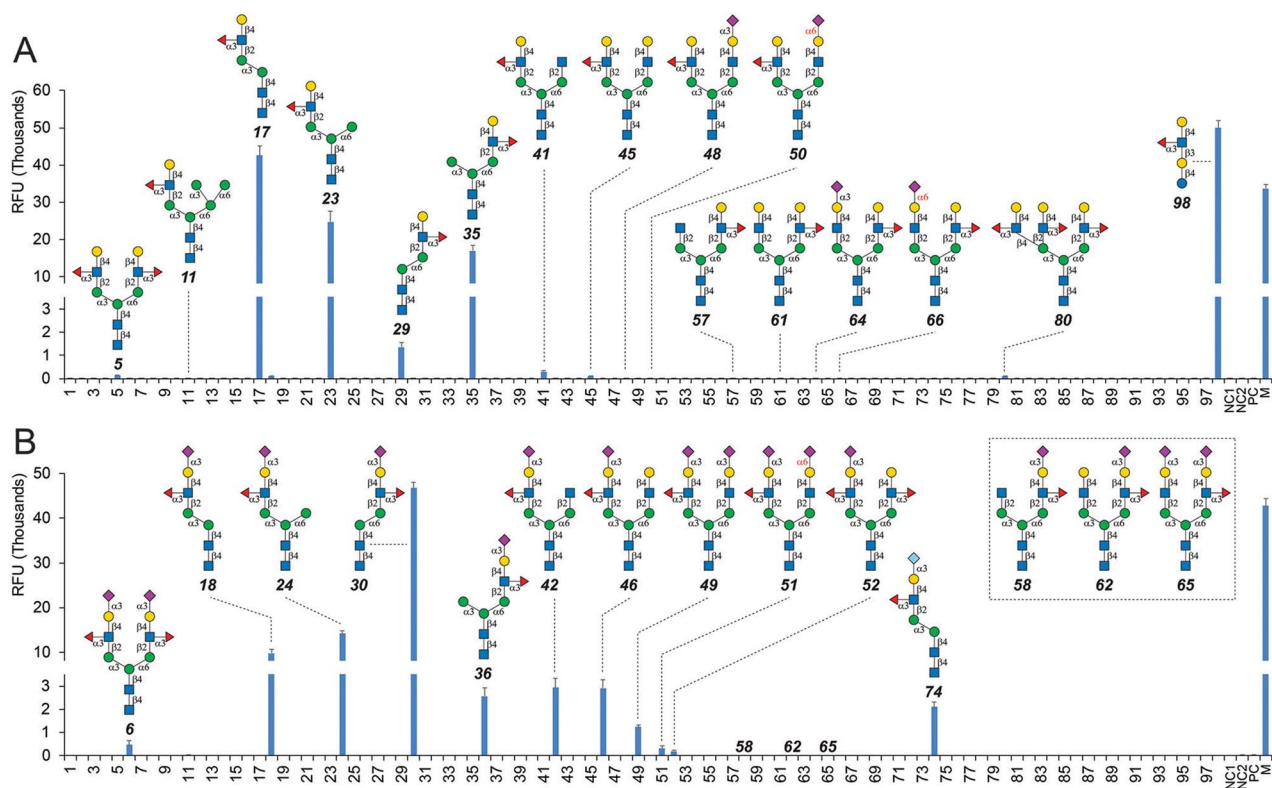


Fig. 5. Selective recognition of *N*-glycans by anti-15CD (A) and anti-15CDs (B) antibodies. Readout by goat anti-mouse IgG–Alexa Fluor 647 conjugate (5 g/mL).

summarized in Table II, one *N*-glycan branch can significantly affect (usually in a negative manner) GBP recognition of the ligand on other branches, depending on the branch length and the modifications it bears. Such a “masking effect” by the opposing branch is GBP-specific, as the binding can change slightly (e.g., AAL), moderately (e.g., SNA), significantly or even be abolished (e.g., anti-CD15 and anti-CD15s antibodies). It should be mentioned that the masking effect may not occur on glycans with elongated branches, (Peng et al. 2017) given likely extended and/or flexible distances between terminal ligands on different branches. Further analyses should be performed using such structures as they are frequently found on mammalian cells especially cancer cells (Pinho et al. 2015). As for same branch modifications, ECL and GS-II cannot tolerate any glycosylation, while AAL and GNL could accommodate α 2,3/-sialylation, α 1,3-fucosylation and β 1,4-galactosylation. Interestingly, RCA-I could only tolerate α 2,6-sialylation when the ligand is located on the α 1,3-Man branch. As reported previously, (Gao et al. 2019) core-fucosylation can be well-tolerated by all tested GBPs.

In summary, protein-glycan interactions contain much more details than their primary binding features, which have been largely ignored. Uncovering such details requires both experimental platforms with massive well-defined glycans to acquire meaningful datasets and algorithms to interpret them. Our glycan microarray with closely related structures and isomers provides valuable insights into fine specificities of GBPs. It is worth noting that all glycoforms are presented in one platform (with AEAB labeling) for comparability, and the specificities may not be well applicable to other platforms (Padler-Karavani et al. 2012). Further analyses using these glycans with other aglycones and on other microarray platforms will be performed in the future.

Materials and methods

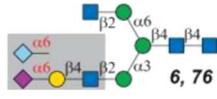
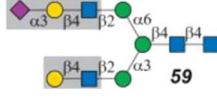
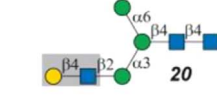
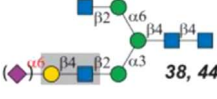
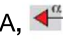
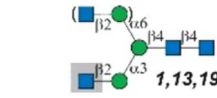
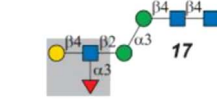
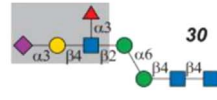
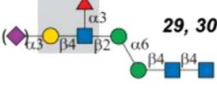
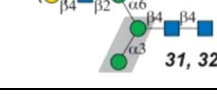
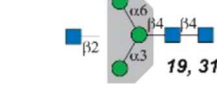
Materials

Biotinylated *Aleuria aurantia* lectin (AAL), Concanavalin A (ConA), *Maaackia amurensis* lectin I (MAL-I), *Sambucus nigra* lectin (SNA) and *Ricinus communis* agglutinin I (RCA-I) were purchased from Vector Laboratories (Burlingame, CA). Biotinylated *Galanthus nivalis* lectin (GNL), *Erythrina cristagalli* lectin (ECL) and *Griffonia simplicifolia* lectin II (GS-II) were purchased from E Y Laboratories (San Mateo, CA). Mouse monoclonal anti-CD15 antibody and biotinylated cholera toxin B subunit (CTB) were purchased from Sigma (St. Louis, MO). The mouse monoclonal anti-CD15s antibody was purchased from Santa Cruz Biotechnology (Dallas, TX). Streptavidin-Cy5 conjugate and goat anti-mouse IgG–Alexa Fluor 647 conjugate were purchased from Thermo Fisher Scientific (Waltham, MA).

Glycan preparation

The majority of *N*-glycans (1–71, 79, and 81–87) and the eight gangliosides were synthesized and purified previously by us (Li et al. 2015; Yu et al. 2016; Calderon et al. 2017). Neu5Gc-terminated *N*-glycans 72–78 were prepared as described previously using one-pot two-enzyme systems, starting with 2, 14 or 28, respectively. The systems contain Neu5Gc, CTP, MgCl₂, *N. meningitidis* CMP-sialic acid synthase (NmCSS) and α 2,3-sialyltransferase 1 mutant E271F/R313Y from *Pasteurella multocida* (PmST1m) or α 2,6-sialyltransferase from *Photobacterium damsela* (Pd2,6ST). Glycan 80 (0.3 mg) was synthesized via the reaction catalyzed by *Helicobacter pylori* α 1,3-fucosyltransferase (Hp3FT) in the presence

Table II. Summary of fine specificities toward *N*-glycans observed in this study. Gray shading indicates the minimum recognition motif (ligand) of corresponding GBPs. Branch preferences, ++ means apparent preference, + means slight preference. NA, not applicable. The symbolic nomenclature for glycans is shown

GBP	Best <i>N</i> -glycan Binder / Ligand (Gray)	Branch Preference	Tolerance of Same Branch Modification				Tolerance of Opposing Branch
			α 2,3-Sia	α 2,6-Sia	α 1,3-Fuc	β 1,4-Gal	
SNA		α 1,3-Man (++)	No	NA (Prefer Neu5Gc)	NA	NA	Yes (Gradient Decrease)
MAL-I		α 1,6-Man (++)	NA (Prefer Neu5Gc)	No	No	NA	Yes (Complicate)
ECL		α 1,3-Man (+)	No	No	No	NA	Yes (if it has not Sia)
RCA-I		α 1,3-Man (++)	No	Yes (If ligand on α 1,3-Man branch)	No	NA	Yes
AAL	NA, 	No	Yes	Yes	Yes	Yes	Yes
GS-II		α 1,3-Man (+)	No	No	No	No	Yes (if has no Sia)
Anti-CD15 Antibody		α 1,3-Man (+)	No	NA	NA	NA	No
Anti-CD15s Antibody		α 1,3-Man (+)	NA	NA	NA	NA	Yes (if ligand is on the α 1,3-Man branch)
CTB		α 1,6-Man (++)	Yes	NA	NA	NA	No
GNL		NA	Yes	Yes	Yes	Yes	Yes
ConA		NA	Tolerate sialylation, fucosylation, galactosylation on both GlcNAc- β 1,2-Man- α 1,3-Man and α 1,6 Man branches; cannot tolerate β 1,4-galactosylation on β 1,4-GlcNAc branch				
Keys: ■ GlcNAc ● Glc ● Gal ● Man ▲ L-Fuc ◆ Neu5Ac ◆ Neu5Gc							

of 79 and GDP-fucose as described before (Li et al. 2015). Glycan 88 (0.1 mg) was synthesized via the bovine α 1,3-galactosyltransferase-catalyzed reaction starting from 14 in the presence of UDP-galactose, as described previously (Wu et al. 2016). Glycan 89 (0.05 mg) was synthesized via the reaction catalyzed by *N. meningitidis* α 1,4-galactosyltransferase (NmLgtC) (Zhang et al. 2002) in the presence of 54 and the sugar donor UDP-galactose. Newly synthesized *N*-glycans were purified by HPLC as described before, (Li et al.

2015) using a Waters XBridge BEH amide column (130 Å, 5 μ m, 10 mm \times 250 mm) under a gradient running condition (solvent A: water or 100 mM ammonium formate; solvent B: acetonitrile; flow rate: 4.5 mL/min, B%: 65–50% in 30 min), monitored by UV absorbance at 210 nm. Product-containing fractions were pooled and lyophilized for mass spectrum (MS) and NMR analysis to confirm structures. Glycan 90 (Man5) was purchased from Sigma.

Glycan derivatization and quantification

All glycans are with free reducing-end and were derivatized by reductive amination using 2-amino-*N*-(2-aminoethyl)-benzamide (AEAB) as previously described (Song et al. 2009). Labeled glycans were further purified by HPLC to homogeneity using a porous graphitic carbon column (5 μ m, 4.6 mm \times 150 mm) under a gradient running condition (solvent A: 0.1% TFA in water; solvent B: 0.1% TFA in acetonitrile; flow rate: 1 mL/min, B%: 15–45% in 30 min), monitored by UV absorbance at 330 nm. Product-containing fractions were pooled and lyophilized for MS characterization. To quantify labeled glycans, 5 mg of AEAB-labeled LNnT was dissolved into various concentrations (1, 5, 10, 20, 50 and 100 μ M), and equal volumes (2 μ L) of each concentration were loaded into HPLC using the porous graphitic carbon column (same condition as described above). A standard curve of peak area vs. concentration was drawn accordingly, and all purified AEAB-labeled glycans were quantified using the standard curve.

Microarray fabrication

The labeled-glycans were prepared at a concentration of 100 μ M in the printing buffer (300 mM phosphate, pH 8.5), and printed on multivalent NHS-derivatized microscope-glass slides (Z Biotech, LLC), each for 400 pL in replicates of six, as described previously (Heimburg-Molinari et al. 2011). Noncontact printing was performed at room temperature with a humidity of 60% by a sciFLEXARRAYER S3 spotter (Sciencion) with two PDC 80 Piezo Dispense Capillary, and eight subarrays were printed on each slide. After overnight dehumidification under room temperature, the slides were washed with MilliQ water and subsequently blocked with 50 mM ethanolamine in 100 mM Tris buffer (pH 9.0) for 2 h. The blocked slides were then washed with MilliQ water twice, dried and stored desiccated at -20°C until use.

Microarray binding assays

Slides were fitted with ProPlate 8-well microarray modules to divide into subarrays and then rehydrated for 10 min with 200 μ L of Buffer TSMTB (20 mM Tris-HCl, pH 7.4, 150 mM NaCl, 2 mM CaCl₂, 2 mM MgCl₂, 0.05% (v/v) Tween-20, 1% (w/v) BSA) at room temperature. Next, the buffer was aspirated and 200 μ L of GBP samples were added into each subarray, sealed and incubated at room temperature for 1 h with gentle shaking. Slides were then washed with Buffer TSMT (20 mM Tris-HCl, pH 7.4, 150 mM NaCl, 2 mM CaCl₂, 2 mM MgCl₂, 0.05% (v/v) Tween-20) four times (3 min per time) and Buffer TSM (20 mM Tris-HCl, pH 7.4, 150 mM NaCl, 2 mM CaCl₂, 2 mM MgCl₂) four times (3 min per time). Next, slides were added with secondary reagents (200 μ L per subarray), sealed and incubated at room temperature for 1 h with gentle shaking. Finally, slides were washed four times each with TSMT, TSM and MilliQ water, respectively, and dried by brief centrifugation. All samples and secondary reagents were dissolved to appropriate concentrations (as shown in Table SI) in Buffer TSMTB. Slides were scanned at 10 μ m resolution with a Genepix 4100A microarray scanner (Molecular Devices Corp., Union City, CA) using 500 or 600 PMT gains and 80% power, and image analyses were carried out with Genepix Pro 6.0 analysis software as previously reported (Padler-Karavani et al. 2012). Spots were defined as circular features with a variable radius as determined by the Genepix scanning software, and local background subtraction was performed. Microarray data resulted from optimal concentrations of each GBP were used to interpret their fine specificities. The optimal concentration of each

GBP (Table SII) was chosen to make sure relative binding values are in the linear range of the scanning instrument.

Supplementary material

Supplementary Material is available at *GLYCOB* online.

Funding

This work was supported by National Institute of General Medical Sciences (U01GM125288 and U01GM116263) and National Heart, Lung, and Blood Institute (U54HL142019).

Declarations of interest

The authors declare that there are no competing interests associated with the manuscript.

Acknowledgments

We are grateful to Z Biotech LLC (Aurora, CO) for printing glycan microarrays (supported by National Institute of Health under R43GM123820) and Dr. Xuezheng Song from Emory University for providing advice and glycan-labeling reagent 2-amino-*N*-(2-aminoethyl)-benzamide (AEAB).

Abbreviations

3'SLN Neu5Ac- α 2,3-LacNAc
 6'SLN Neu5Ac- α 2,6-LacNAc
 AEAB 2-amino-*N*-(2-aminoethyl)-benzamide
 Fuc L-fucose
 Gal galactose
 GBP glycan-binding protein
 GlcNAc *N*-acetylglucosamine
 LacNAc Gal- β 1,4-GlcNAc
 Le^x Gal- β 1,4-(Fuc- α 1,3-)GlcNAc
 Man mannose
 Neu5Ac *N*-acetylneuraminic acid
 Neu5Gc *N*-glycolylneuraminic acid
 NHS *N*-hydroxysuccinimide
 Sia sialic acid
 sLe^x Neu5Ac- α 2,3-Gal- β 1,4-(Fuc- α 1,3-)GlcNAc
 TFA trifluoroacetic acid

References

- Agravat SB, Saltz JH, Cummings RD, Smith DF. 2014. GlycoPattern: A web platform for glycan array mining. *Bioinformatics*. 30:3417–3418.
- Ban L, Pettit N, Li L, Stuparu AD, Cai L, Chen W, Guan W, Han W, Wang PG, Mrksich M. 2012. Discovery of glycosyltransferases using carbohydrate arrays and mass spectrometry. *Nat Chem Biol*. 8:769–773.
- Calderon AD, Liu Y, Li X, Wang X, Chen X, Li L, Wang PG. 2016. Substrate specificity of FUT8 and chemoenzymatic synthesis of core-fucosylated asymmetric N-glycans. *Org Biomol Chem*. 14:4027–4031.
- Calderon AD, Zhou J, Guan W, Wu Z, Guo Y, Bai J, Li Q, Wang PG, Fang J, Li L. 2017. An enzymatic strategy to asymmetrically branched N-glycans. *Org Biomol Chem*. 15:7258–7262.
- Echeverria B, Serna S, Achilli S, Vives C, Pham J, Thepaut M, Hokke CH, Fieschi F, Reichardt NC. 2018. Chemoenzymatic synthesis of N-glycan positional isomers and evidence for branch selective binding by monoclonal antibodies and human C-type Lectin receptors. *ACS Chem Biol*. 13:2269–2279.

- Fang J, Li J, Chen X, Zhang Y, Wang J, Guo Z, Zhang W, Yu L, Brew K, Wang PG. 1998. Highly efficient chemoenzymatic synthesis of alpha-galactosyl epitopes with a recombinant alpha-(1->3)-galactosyltransferase. *J Am Chem Soc.* 120:6635–6638.
- Gao C, Hanes MS, Byrd-Leotis LA, Wei M, Jia N, Kardish RJ, McKittrick TR, Steinhauer DA, Cummings RD. 2019. Unique binding specificities of proteins toward isomeric asparagine-linked Glycans. *Cell Chem Biol.* 26:535:e534–e547.
- Grant OC, Tessier MB, Meche L, Mahal LK, Foley BL, Woods RJ. 2016. Combining 3D structure with glycan array data provides insight into the origin of glycan specificity. *Glycobiology.* 26:772–783.
- Heimburg-Molinari J, Song X, Smith DF, Cummings RD. 2011. Preparation and analysis of glycan microarrays. *Curr Protoc Protein Sci.* Chapter 12:Unit12 10.
- Hendrickson OD, Zherdev AV. 2018. Analytical application of Lectins. *Crit Rev Anal Chem.* 48:279–292.
- Hirabayashi J, Kuno A, Tateno H. 2015. Development and applications of the Lectin microarray. *Top Curr Chem.* 367:105–124.
- Hudak JE, Bertozzi CR. 2014. Glycotherapy: New advances inspire a reemergence of glycans in medicine. *Chem Biol.* 21:16–37.
- Itakura Y, Nakamura-Tsuruta S, Kominami J, Sharon N, Kasai K, Hirabayashi J. 2007. Systematic comparison of oligosaccharide specificity of Ricinus communis agglutinin I and Erythrina lectins: A search by frontal affinity chromatography. *J Biochem.* 142:459–469.
- Kim CS, Seo JH, Cha HJ. 2012. Functional interaction analysis of GM1-related carbohydrates and vibrio cholerae toxins using carbohydrate microarray. *Anal Chem.* 84:6884–6890.
- Klamer Z, Staal B, Prudden AR, Liu L, Smith DF, Boons GJ, Haab B. 2017. Mining high-complexity motifs in Glycans: A new language to uncover the fine specificities of Lectins and Glycosidases. *Anal Chem.* 89:12342–12350.
- Kletter D, Singh S, Bern M, Haab BB. 2013. Global comparisons of lectin-glycan interactions using a database of analyzed glycan array data. *Mol Cell Proteomics.* 12:1026–1035.
- Kuno A, Uchiyama N, Koseki-Kuno S, Ebe Y, Takashima S, Yamada M, Hirabayashi J. 2005. Evanescent-field fluorescence-assisted lectin microarray: A new strategy for glycan profiling. *Nat Methods.* 2:851–856.
- Li L, Liu Y, Ma C, Qu J, Calderon AD, Wu B, Wei N, Wang X, Guo Y, Xiao Z et al. 2015. Efficient chemoenzymatic synthesis of an N-glycan isomer library. *Chem Sci.* 6:5652–5661.
- Liu Y, McBride R, Stoll M, Palma AS, Silva L, Agravat S, Aoki-Kinoshita KF, Campbell MP, Costello CE, Dell A et al. 2016. The minimum information required for a glycomics experiment (MIRAGE) project: Improving the standards for reporting glycan microarray-based data. *Glycobiology.* 27:280–284
- Maupin KA, Liden D, Haab BB. 2012. The fine specificity of mannose-binding and galactose-binding lectins revealed using outlier motif analysis of glycan array data. *Glycobiology.* 22:160–169.
- Padler-Karavani V, Song X, Yu H, Hurtado-Ziola N, Huang S, Muthana S, Chokhawala HA, Cheng J, Verhagen A, Langereis MA et al. 2012. Cross-comparison of protein recognition of sialic acid diversity on two novel sialoglycan microarrays. *J Biol Chem.* 287:22593–22608.
- Peng W, de Vries RP, Grant OC, Thompson AJ, McBride R, Tsogtbaatar B, Lee PS, Razi N, Wilson IA, Woods RJ et al. 2017. Recent H3N2 viruses have evolved specificity for extended, branched human-type receptors, conferring potential for increased avidity. *Cell Host Microbe.* 21:23–34.
- Pilobello KT, Krishnamoorthy L, Slawek D, Mahal LK. 2005. Development of a lectin microarray for the rapid analysis of protein glycopatterns. *Chembiochem.* 6:985–989.
- Pilobello KT, Slawek DE, Mahal LK. 2007. A ratiometric lectin microarray approach to analysis of the dynamic mammalian glycome. *Proc Natl Acad Sci U S A.* 104:11534–11539.
- Pinho SS, Reis CA. 2015. Glycosylation in cancer: Mechanisms and clinical implications. *Nat Rev Cancer.* 15:540–555.
- Porter A, Yue T, Heeringa L, Day S, Suh E, Haab BB. 2010. A motif-based analysis of glycan array data to determine the specificities of glycan-binding proteins. *Glycobiology.* 20:369–380.
- Rodríguez E, Schetters STT, van Kooyk Y. 2018. The tumour glyco-code as a novel immune checkpoint for immunotherapy. *Nat Rev Immunol.* 18:204–211.
- Shibuya N, Goldstein IJ, Van Damme EJ, Peumans WJ. 1988. Binding properties of a mannose-specific lectin from the snowdrop (*Galanthus nivalis*) bulb. *J Biol Chem.* 263:728–734.
- Shivatere SS, Chang SH, Tsai TI, Tseng SY, Shivatere VS, Lin YS, Cheng YY, Ren CT, Lee CC, Pawar S et al. 2016. Modular synthesis of N-glycans and arrays for the hetero-ligand binding analysis of HIV antibodies. *Nat Chem.* 8:338–346.
- Smith DF, Song X, Cummings RD. 2010. Use of glycan microarrays to explore specificity of glycan-binding proteins. In: *Methods in enzymology.* San Diego, CA: Elsevier. p. 417–444.
- Song X, Xia B, Stowell SR, Lasanajak Y, Smith DF, Cummings RD. 2009. Novel fluorescent glycan microarray strategy reveals ligands for galectins. *Chem Biol.* 16:36–47.
- Song X, Yu H, Chen X, Lasanajak Y, Tappert MM, Air GM, Tiwari VK, Cao H, Chokhawala HA, Zheng H et al. 2011. A sialylated glycan microarray reveals novel interactions of modified sialic acids with proteins and viruses. *J Biol Chem.* 286:31610–31622.
- Taylor ME, Drickamer K. 2009. Structural insights into what glycan arrays tell us about how glycan-binding proteins interact with their ligands. *Glycobiology.* 19:1155–1162.
- Taylor ME, Drickamer K, Schnaar RL, Etzler ME, Varki A. 2015. Discovery and classification of glycan-binding proteins. In: Varki A, Cummings RD, Esko JD, Stanley P, Hart GW, Aebi M, Darvill AG, Kinoshita T, Packer NH et al., editors. *Essentials of glycobiology.* 3rd ed. New York: Cold Spring Harbor. p. 361–372.
- Wands AM, Fujita A, McCombs JE, Cervin J, Dedic B, Rodriguez AC, Nischan N, Bond MR, Mettlen M, Trudgian DC et al. 2015. Fucosylation and protein glycosylation create functional receptors for cholera toxin. *Elife.* 4:e09545.
- Wang L, Cummings RD, Smith DF, Huflejt M, Campbell CT, Gildersleeve JC, Gerlach JQ, Kilcoyne M, Joshi L, Serna S et al. 2014. Cross-platform comparison of glycan microarray formats. *Glycobiology.* 24: 507–517.
- Wang S, Zhang Q, Chen C, Guo Y, Gadi MR, Yu J, Westerlind U, Liu Y, Cao X, Wang PG et al. 2018. Facile chemoenzymatic synthesis of O-mannosyl glycans. *Angew Chem Int Ed Engl.* 57:9268–9273.
- Wang WC, Cummings RD. 1988. The immobilized leucoagglutinin from the seeds of *Maackia amurensis* binds with high affinity to complex-type Asn-linked oligosaccharides containing terminal sialic acid-linked alpha-2,3 to penultimate galactose residues. *J Biol Chem.* 263:4576–4585.
- Wang Z, Chinoy ZS, Ambre SG, Peng W, McBride R, de Vries RP, Glushka J, Paulson JC, Boons GJ. 2013. A general strategy for the chemoenzymatic synthesis of asymmetrically branched N-glycans. *Science.* 341:379–383.
- Wu AM, Wu JH, Tsai MS, Yang Z, Sharon N, Herp A. 2007. Differential affinities of Erythrina cristagalli lectin (ECL) toward monosaccharides and polyvalent mammalian structural units. *Glycoconj J.* 24: 591–604.
- Wu Z, Liu Y, Li L, Wan XF, Zhu H, Guo Y, Wei M, Guan W, Wang PG. 2017. Decoding glycan protein interactions by a new class of asymmetric N-glycans. *Org Biomol Chem.* 15:8946–8951.
- Wu Z, Liu Y, Ma C, Li L, Bai J, Byrd-Leotis L, Lasanajak Y, Guo Y, Wen L, Zhu H et al. 2016. Identification of the binding roles of terminal and internal glycan epitopes using enzymatically synthesized N-glycans containing tandem epitopes. *Org Biomol Chem.* 14: 11106–11116.
- Xuan P, Zhang Y, Tzeng TR, Wan XF, Luo F. 2012. A quantitative structure-activity relationship (QSAR) study on glycan array data to determine the specificities of glycan-binding proteins. *Glycobiology.* 22:552–560.
- Yu H, Li Y, Zeng J, Thon V, Nguyen DM, Ly T, Kuang HY, Ngo A, Chen X. 2016. Sequential one-pot multienzyme chemoenzymatic synthesis of glycosphingolipid glycans. *J Org Chem.* 81:10809–10824.
- Zhang J, Kowal P, Fang J, Andrea P, Wang PG. 2002. Efficient chemoenzymatic synthesis of globotriose and its derivatives with a recombinant alpha-(1->4)-galactosyltransferase. *Carbohydr Res.* 337:969–976.

- Zhang L, Luo S, Zhang B. 2016. The use of lectin microarray for assessing glycosylation of therapeutic proteins. *MAbs*. 8:524–535.
- Zhao N, Martin BE, Yang CK, Luo F, Wan XF. 2015. Association analyses of large-scale glycan microarray data reveal novel host-specific substructures in influenza A virus binding glycans. *Sci Rep*. 5: 15778.
- Zhu K, Bressan RA, Hasegawa PM, Murdock LL. 1996. Identification of N-acetylglucosamine binding residues in *Griffonia simplicifolia* lectin II. *FEBS Letters*. 390:271–274.
- Zou X, Yoshida M, Nagai-Okatani C, Iwaki J, Matsuda A, Tan B, Hagiwara K, Sato T, Itakura Y, Noro E *et al.* 2017. A standardized method for lectin microarray-based tissue glycome mapping. *Sci Rep*. 7:43560.